



The investigation of structure–activity relationship of polyamine-targeted synthetic compounds from different chemical groups

Sergey P. Syatkin¹ · Ekaterina V. Neborak¹ · Andrei I. Khlebnikov^{2,3} · Marina V. Komarova⁴ · Natalia A. Shevkun⁵ · Eduard G. Kravtsov¹ · Mikhail L. Blagoravov¹ · Enzo Agostinelli^{6,7}

Received: 11 March 2019 / Accepted: 14 August 2019 / Published online: 13 September 2019
© Springer-Verlag GmbH Austria, part of Springer Nature 2019

Abstract

The polyamine (PA) metabolism is involved in cell proliferation and differentiation. Increased cellular PA levels are observed in different types of cancers. Products of PA oxidation induce apoptosis in cancer cells. These observations open a perspective to exploit the enzymes of PA catabolism as a target for anticancer drug design. The substances capable to enhance PA oxidation may become potential anticancer agents. The goal of our study was to explore how the mode of ligand binding with a PA catabolic enzyme is associated with its stimulatory or inhibitory effect upon PA oxidation. Murine *N1*-acetylpolyamine oxidase (5LFO) crystalline structure was used for molecular docking with ligands of various chemical structures. In vitro experiments were carried out to evaluate the action of the tested compounds upon PA oxidative deamination in a cell-free test system from rat liver. Two amino acid residues (Aps211 and Tyr204) in the structure of 5LFO were found to be significant for binding with the tested compounds. 19 out of 51 screened compounds were activators and 17 were inhibitors of oxidative deamination of PA. Taken together, these results enabled to construct a recognition model with characteristic descriptors depicting activators and inhibitors. The general tendency indicated that a strong interaction with Asp211 or Tyr204 was rather typical for activators. The understanding of how the structure determines the binding mode of compounds with PA catabolic enzyme may help in explanation of their structure–activity relationship and thus promote structure-based drug design.

Keywords Polyamines · Polyamine catabolism · Polyamine-targeted agents · Molecular docking · Structure–activity relationship

Abbreviations

AA Amino acid
APAO *N*-acetylpolyamine oxidase

BENSpm Bis(ethyl)norspermine
CPENSpm *N1*-cyclopropylmethyl-*N1*-ethylnorspermine
FAD Flavine adenine dinucleotide
N1-acetyl-Spm *N1*-acetylspermine
PA(s) Polyamine(s)
PAO Polyamine oxidase
PDB Protein Data Bank

Handling Editor: E. Closs.

Electronic supplementary material The online version of this article (<https://doi.org/10.1007/s00726-019-02778-3>) contains supplementary material, which is available to authorized users.

✉ Sergey P. Syatkin
syatkin_sp@pfur.ru; syata@mail.ru

¹ Medical Institute, RUDN University (Peoples' Friendship University of Russia), Miklukho-Maklaya str.6, Moscow 117198, Russia

² Kizhner Research Center, National Research Tomsk Polytechnic University, Tomsk 634050, Russia

³ Scientific Research Institute of Biological Medicine, Altai State University, Barnaul 656049, Russia

⁴ Samara University, Moskovskoye shosse, 34, Samara 443086, Russia

⁵ Drug Product Division, Project Development Department, NEARMEDIC PHARMA LLC, Moscow, Russia

⁶ Department of Biochemical Sciences, SAPIENZA University of Rome, Piazzale Aldo Moro 5, 00185 Rome, Italy

⁷ International Polyamines Foundation, ONLUS, Via del Forte Tiburtino, 98, 00159 Rome, Italy

SMO	Spermine oxidase
SSAT	Spermine/spermidine- <i>N</i> -acetyltransferase
Spm	Spermine
Spd	Spermidine
MDL 72527	<i>N</i> 1, <i>N</i> 4-bis(2,3-butadienyl)-1,4-butanediamine dihydrochloride

Introduction

Polyamines (PA)–spermidine (Spd) and spermine (Spm) are organic polycations. They are found practically in all living organisms and are important regulators of cell growth, differentiation, and apoptosis (Miller-Fleming et al. 2015). Disturbances in their metabolism resulting in increased PA concentrations accompany accelerated cell proliferation and occur in a variety of cancers and pathophysiological conditions. Antineoplastic agents were shown to normalize PA metabolism in tumor cells (Casero et al. 2005; Murray-Stewart et al. 2017). Thus, PA metabolism can serve as a therapeutic target. The excess of PA inside a transformed cell during carcinogenesis is in many cases due not only to a significant activation of their synthesis but also to reduction or total suppression of PA catabolism through oxidative deamination (Syatkin and Berezov 1982; Wallace et al. 2000), while the products of their catabolism (iminoaldehydes and H₂O₂) cause apoptosis and show anticancer and antimicrobial activity, inhibit the growth of some types of cancer cells, bacteria, and viruses (Amendola et al. 2013; Moschou and Roubelakis-Angelakis 2014; Grancara et al. 2015). Moreover, it is well documented that the activity of PA catabolic enzymes is sharply lowered in different cancer tissues (Wallace et al. 2000; Cervelli et al. 2014; Syatkin et al. 2017). These facts indicate the significance of PA catabolic pathway for restoration of the control mechanism of cellular proliferation.

Recently synthetic analogues of PA were found to affect PA metabolic pathway in such a way that the rate of their catabolism exceeds the rate of their synthesis. The cytotoxic agents are formed thereby ultimately blocking the malignant proliferation (Obakan et al. 2014a, b). Three enzymes are known to be responsible for PA degradation in mammals: Spm/Spd-*N*-acetyltransferase (SSAT), *N*1-acetylpolyamine oxidase (APAO), and Spm oxidase (SMO). In detail, PA metabolism is discussed in lots of recent reviews (Casero et al. 2005; Miller-Fleming et al. 2015; Murray-Stewart et al. 2017). Observations prove that PA catabolic enzymes may contribute to apoptosis induction (Tavladoraki et al. 2012; Wang et al. 2015; Wang et al. 2017). Various PA analogues are known to demonstrate antiproliferative activity by inducing and stabilizing PA catabolic enzymes (Thomas and Thomas 2018). This approach appears to be promising for

development of potential anticancer agents among activators of PA catabolism.

Until now, screening remains the initial stage in searching of biologically active compounds. The structure-based drug design requires information about the properties of compounds, which could enable the researcher to predict type of activity based on structural features of similar compounds. These data are also useful for optimization of substituting and functional groups in the series of similar compounds (compound libraries) during the so-called lead optimization (Anderson 2012; Kaur et al. 2016). For these purposes, bioinformatics and computer modeling technologies, such as molecular docking, are widely used (Sliwoski et al. 2013; Battu et al. 2014; Vucicevic et al. 2017).

In the present study, we report the development of a classification tree for 36 nitrogen-containing substances with different chemical structures built on the basis of docking data together with their *in vitro* activity. Initially, 51 new organic compounds were explored for their ability to influence the PA metabolism. After that, molecular docking was implemented to reveal the binding sites of ligands (tested compounds) with the target enzyme. Molecular docking requires 3D structure of a protein and homology modeling is often used in its absence (Samasil et al. 2017). Our *in vitro* investigations were performed in rats, but no crystal structure of PA catabolic enzymes has been described for this animal. The recently described murine APAO (Sjögren et al. 2017) was chosen for docking simulation as the most suitable model protein. Two amino acid (AA) residues were identified as significant ones for ligand–protein interaction. The classification and regression tree analysis (C&RT) was applied to build a recognition model for distinction between activators and inhibitors among the tested ligands.

Materials and methods

Tested compounds

All the tested compounds were gained from the Department of Organic Chemistry of PFUR where they were synthesized as described previously (Anh et al. 2004, 2012a, b, c; Volkov et al. 2007; Hieu et al. 2012a, b, 2013). All the compounds were divided into eight groups according to their chemical structure. These were aniline, dioxaborinopyridine, azaflorene, azacrown ether with *N*-containing aliphatic heterocycle and without it, benzobicyclononane, diphenylpiperidine, and bacteriopurpurin derivatives (see Table 1).

Reagents

Putrescine-2HCl, Spd-3HCl, and Spm-4HCl were from Fluka (Switzerland). *O*-dianisidine hydrochloride, 30%

Table 1 The groups of the tested compounds

Group	Chemical basic structure	Number of compounds	Number of activators ^a
I	Aniline	14	7
II	Dioxaborinopyridine	12	3
III	Azafluorene	4	4
IV	Azacrown ethers with N-containing aliphatic heterocycle	8	0
V	Azacrown ethers of different structures	3	1
VI	Benzobicyclononane	2	2
VII	Diphenylpiperidine	4	2
VIII	Bacteriopurpurin	4	0
Total		51	19

^aThe number of compounds classified as true (not ambivalent) activators of PA catabolism

hydrogen peroxide, and horseradish peroxidase (150 U/mg), and Tris–HCl were produced by Sigma. All the reagents for Bradford method were purchased from Sigma-Aldrich. The tested substances were diluted in 50 mM Tris–HCl buffer with 1% DMSO.

Cell-free test system

The supernatant of liver homogenate of healthy Sprague–Dawley rats was used as a source of the enzymes. The liver tissue was mechanically homogenized with an Omni MultiMix200 homogenizer (Omni Inc., USA) in nine parts (w/v) of a cold 50 mM Tris–HCl buffer pH = 9.0 containing 0.05% SDS and a mixture of protease inhibitors. The supernatant of the 33% homogenate obtained after centrifugation at 10,000 g for 20 min (5417R, “Eppendorf”) was a postmitochondrial fraction. The experiments with the animals were carried out according to the protocols approved by the Ethic Committee of PFUR.

Enzyme assay

Determination of amine oxidases activity in vitro was performed by a modified spectrophotometric method (Syatkin and Galaev 1977; Storer and Ferrante 1998). The supernatant of 10% liver homogenate in Tris buffer solution was preincubated in 96-well plates for 1 h at 37 °C with peroxidase in the presence of 100 μM test compounds (the general scheme—see Table S1 in the Supplementary material). *O*-dianisidine and Spd-3HCl and Spm-4HCl were then added. The final concentration of the substrates was 10.7 μM. The mixture was incubated again for 30 min, and the absorption was measured at 540 nm, the colored product being formed by oxidation of *O*-dianisidine with hydrogen peroxide evolved in the amine oxidase reaction. The control

samples contained all the same components except the tested compounds. Additional control samples contained all the same components except substrates and their values were subtracted from the experimental ones, so that any kind of unspecific influence of the compounds on the test system itself was excluded. The data are presented as the mean for three independent experiments.

Protein assay

The protein concentration in the supernatant was determined by the Bradford method (Bradford 1976).

Molecular docking

The only one mammalian PAO namely murine APAO (PAOX_MOUSE) is available in Protein Data Bank (PDB) with its crystal structure. We performed the alignment using the online service Clustal Omega (Madeira et al. 2019) at the site <https://www.uniprot.org> and found out that it shares 62.5% similarity with human APAO and 79.8% with rat APAO (Supplementary Material, Fig. S1, S2); therefore, it was considered a suitable model protein and used for docking investigation. Molecular model of 5LFO in complex with its substrate *N*1-acetylspermine (*N*1-acetyl-Spm) and coenzyme FAD (Sjögren et al. 2017) was downloaded from PDB. The model was imported into Molegro Virtual Docker (MVD) program, Version 6.0. The search space for docking was chosen as a sphere with 12 Å radius placed at the geometric center of gravity of the co-crystallized substrate. The spherical search space completely encompassed the co-crystallized ligand and the 5LFO-binding site. Side chains of 60 residues closest to substrate molecule were considered flexible during docking. FAD molecule was regarded as a rigid cofactor on the calculations. Structures of all the investigated compounds (ligands) were built with the use of ChemBioOffice 2010 software and pre-optimized by semi-empirical PM3 method with HyperChem 7 program. The compound structures were imported in MVD and docked into the binding site of 5LFO with full conformational flexibility of ligands and side chains of the above-mentioned AA residues. The flexible residues were treated with default settings of “Setup Sidechain Flexibility” tool in MVD, and a softening parameter of 0.7 was applied during flexible docking, according to the standard protocol using MVD program. Fifteen docking runs were performed for each compound with MolDock scoring function. Conformation with the lowest docking score was analyzed for each ligand. Using the “Energy inspector” option, the partial energies of ligand–residue interactions were extracted from the overall docking score.

The classification tree building

SPSS 21 software was used for statistical analysis. As the data did not belong to the Gaussian distribution model, non-parametrical methods were applied. Comparisons between groups of activators, inhibitors, and ambivalent compounds were performed using Kruskal–Wallis rank sum test and the Mann–Whitney *U* test with correction for multiple testing according to Bonferroni method. Spearman correlation coefficients were calculated to evaluate associations between energies of ligand–residue interactions and activity of each compound which was coded as –1—Inhibitor, 0—NA, 1—Activator. Continuous variables were described as median and interquartile range Me (IQR).

To find combinations of descriptors of docking providing activation or inhibition effect, classification tree was built according to C&RT algorithm (Khlebnikov et al. 2012). Only those compounds that showed an unequivocal (not ambivalent) influence on oxidation of PA were taken for classification tree building. Selection of best attributes was based on Gini index. To reduce redundant attributes and to remove the unreliable branches, limitation for parent node size was set as 19 and for child node as five. We did not use validation of the classification tree by dividing data into training and testing sets because of relatively small amount of studied substances with quite different chemical structure. Also, an ROC curve was constructed. For all statistical tests, $P < 0.05$ was considered significant.

Results and discussion

Oxidative deamination assay

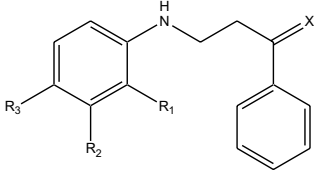
Commonly, 51 compounds from eight different chemical groups were screened for their ability to affect PA oxidation. In general, 19 compounds were activators of PA catabolism, 17 compounds were inhibitors, and the rest 15 gave an ambivalent effect on oxidation of Spd and Spm.

A common pathway for oxidation of Spd and Spm includes two enzymes. Initially, SSAT acetylates both PAs, and then, APAO converts acetylated substrates into putrescine and Spd, respectively. An alternative mechanism of oxidation is known for Spm. SMO, the third PA catabolic enzyme, oxidizes Spm into Spd without intermediate acetylation step. To summarize, the PA oxidation can occur by two pathways either with one enzyme performing a direct oxidation of Spm (SMO) or with two enzymes (SSAT and APAO) involved in oxidation of both Spd and Spm through intermediate acetylated forms. Due to financial limitations, only non-acetylated PAs were used in this work. Thus, the results presented in this study show the influence of the tested compounds upon oxidative deamination of free PAs.

Our cell-free test system contained all the enzymes of PA catabolism due to its origin. As Spm is the substrate for both SMO and SSAT, hydrogen peroxide, the final product of PA oxidation that was exploited for the detection of amine oxidase activity may originate from both the mentioned pathways. Although SSAT and SMO are cytosolic enzymes, the SSAT substrate affinity for Spm is more than 30 times higher than that of SMO, as demonstrated by their K_m values (Adachi et al. 2010; Miller-Fleming et al. 2015). Rapid covering of polar positively charged amino group with an acetyl group by SSAT may contribute to predominant utilization of Spm (in its acetylated form) by APAO, but not by SMO. At the same time, Spd also produces hydrogen peroxide by SSAT-APAO pathway. All this supported the reason for developing a classification tree on the data obtained for both substrates—Spd and Spm. A compound was evaluated as an activator if it activated oxidation of both Spd and Spm or at least one of them without decreasing oxidation of the second one. In case of ambivalent effect, a compound was considered belonging to “Not applied” (NA) category. The results are presented as a mean for three independent repetitions.

Group I: Seven compounds of aniline derivatives turned out to be activators and four of them—inhibitors of PA catabolism. The structures of all these compounds differ by the type of radical in the aniline ring, and the B14 also has a hydrazine group instead of a keto-group (see Table 2). All the compounds with a halogen in aniline ring regardless of its position inside of the ring activated oxidation of PA. The strongest activators were fluoro-substituted B8 and B9. Inhibitors are the unsubstituted compound itself (B1), the agents with methyl-radical (B2), nitro-group (B11), and those with methoxymethyl- (B12) and ethoxycarbonyl-groups (B13). It is worth noticing that the compounds of this group are similar to the structure of resveratrol as they also contain two aromatic rings linked with a carbon chain. Resveratrol was revealed to affect the PA metabolism (Handa et al. 2018); therefore, the similarity of structure may be a key in deeper understanding of structure–activity relationship. The fact that the highest activation was observed for fluorinated derivatives supports the tradition of fluorine application in medicinal chemistry (Meanwell 2018).

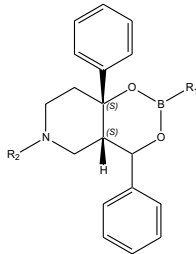
Group II: Derivatives of dioxaborinopyridine mainly act as inhibitors of PA oxidative deamination (Table 3) with the most pronounced action observed towards the oxidation of Spm. However, adding the compounds CoA2, CoA3, and CoA5 enhanced the process of oxidative deamination of Spd. CoA5 activates oxidation of both the substrates. We earlier tested the compounds of similar structure (Syatkin et al. 2017) and showed that anilines are capable to activate PA catabolism, while dioxaborinopyridines may inhibit it. Therefore, our current results support these previously gained data.

Table 2 Structures of aniline derivatives (group I) and their influence on amine oxidase activity in a cell-free test system from rat liver


Group I

Code	X	R1	R2	R3	Oxidative deamination of Spd		Oxidative deamination of Spm		Observed Category
					nkatal/mg of protein	%	nkatal/mg of protein	%	
B1	O	H	H	H	10	56	9	90	Inhibitor
B2	O	H	H	Me	14	78	7	70	Inhibitor
B3	O	H	H	Et	18	100	17	170	NA
B4	O	H	H	iPr	28	156	19	190	Activator
B5	O	H	H	Cl	32	178	22	220	Activator
B6	O	H	H	Br	28	156	20	200	Activator
B7	O	H	H	J	31	172	11	110	Activator
B8	O	F	H	H	35	194	29	290	Activator
B9	O	H	CF ₃	H	30	167	31	310	Activator
B10	O	H	Cl	H	18	100	13	130	NA
B11	O	H	NO ₂	H	11	61	8	80	Inhibitor
B12	O	H	H	COOEt	12	67	9	90	Inhibitor
B13	O	H	H	CH ₂ OMe	16	89	11	110	NA
B14	N=NH	Cl	H	H	23	128	16	160	Activator

The data are presented as the mean for three independent experiments

Table 3 Structures of dioxaborinopyridine derivatives (group II) and their influence on amine oxidase activity in a cell-free test system from rat liver


Group II
*) Chiral centers: 4, 4a, 8a – R, S, S

Code	R1	R2	Oxidative deamination of Spd		Oxidative deamination of Spm		Observed Category
			nkatal/mg of protein	(%)	nkatal/mg of protein	(%)	
CoA1	2-methylphenyl	Methyl	16	123	17	142	Activator
CoA2	2-methyl-4-methoxyphenyl	Methyl	17	131	10	83	NA
CoA3	2,4,6-trimethylphenyl	Methyl	19	146	7	58	NA
CoA4	3-trifluoromethylphenyl	Methyl	10	77	12	100	NA
CoA5	2-thienyl	Methyl	19	146	15	125	Activator
CoA6	phenyl	Methyl	9	69	8	67	Inhibitor
CoA7	3-fluoro-4-chlorophenyl	Methyl	13	100	16	133	NA
CoA8	3-methylphenyl	Methyl	8	62	6	50	Inhibitor
CoA9	4-methylphenyl	Methyl	4	31	4	33	Inhibitor
CoA10	4-cyanophenyl	Methyl	11	85	13	108	NA
CoA11	4-methylphenyl	Benzyl	15	115	14	117	Activator
CoA12	phenyl	Benzyl	7	54	5	42	Inhibitor

Group III: All the azafluorenes activate PA oxidation, due to the strongest activator F1 (Table 4). This structure contains a keto-group in position 9 and no halogens in the pyridine ring. Bromination of the pyridine ring as well as adding a phenylimino group into position 9 slightly reduces the activating effect of the tested azafluorenes on PA oxidation. We found in literature some bis-indole alkaloids from *Arundo Donax* and cyathocaline–isoursoline from *Pseuduvaria fragrans* with structures resembling the currently tested azafluorenes. There is little information about these compounds, but among other kinds of biological activities, they were shown to possess antiproliferative effects (Panidthanon et al. 2018; Reinus and Kerwin 2019).

Group IV: No true activators of PA catabolism were found among azacrown ethers with N-containing aliphatic heterocycle (Table 4). Sulfur- and iminogroup-containing agents X1, X2, X4, and X5 were true inhibitors, whereas other four compounds showed ambivalent action. The

degree of inhibition goes down in the row of substituents allyl-, methyl-, and H- for S-containing agents. The replacement of =S with NH= group also reduces the inhibitory effect of this molecule.

Group V: This group (Table 5) presents the greatest variety of structures. It has given us one activator namely X17 that is an azacrown macro-ring with additional pyridine cycle. Comparing this compound with the previous group of structures, one can easily see that the main differences lay in total aromaticity of the azacrown cycle and this additional pyridine cycle. Therefore, these features give us the relationship with the activatory effect of this compound. The similar structure (X11), but consisting of two azacrown macro-rings, mutually connected by a phenylene bridge inhibited deamination of PAs. The X10 compound, that is a nitrogen-free macrocyclic (28 atoms) azacrown ether, enhanced slightly oxidation of

Table 4 Structures of azafluorene (group III) and azacrown ether (group IV) derivatives and their influence on amine oxidase activity in a cell-free test system from rat liver

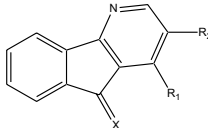
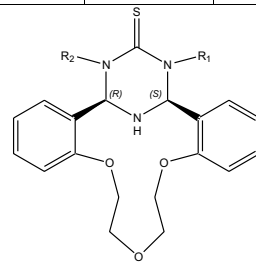
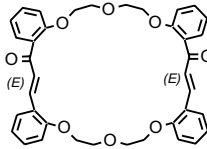
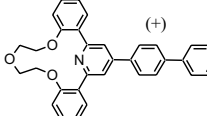
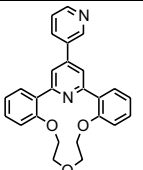
										
Group III										
Code	X	R ₁	R ₂	Oxidative deamination of Spd		Oxidative deamination of Spm		Observed Category		
				nkatal/mg of protein	(%)	nkatal/mg of protein	(%)			
F1	O	NH ₂	H	40	143	31	207	Activator		
F2	-NH-Phenyl	NH ₂	H	38	136	27	180	Activator		
F3	O	Br	H	35	125	29	193	Activator		
F4	O	NH ₂	Br	41	146	20	133	Activator		
										
Group IV										
Code	X	Y	=Z (-Z)	R ₁	R ₂	Oxidative deamination of Spd		Oxidative deamination of Spm		Observed Category
						nkatal/mg of protein	(%)	nkatal/mg of protein	(%)	
X1	N	N	=S	Allyl	H	9,9	34	9	60	Inhibitor
X2	N	N	=S	Me	H	14,5	50	7	47	Inhibitor
X4	N	N	=S	H	H	17,5	60	9	60	Inhibitor
X5	N	N	=N H	H	H	19,8	68	12	80	Inhibitor
X6	C	N	=O	Carbamoyl	H	24	83	15,5	103	NA
X14	C	C	-OH	Phenyl	Phenyl	21,5	74	17,2	115	NA
X19	C	C	=O	COOMe	-COOMe	12	41	16,3	109	NA
X20	C	C	-OH	COOMe	H	28,8	99	33	220	NA

Table 5 Structures of group V compounds and their influence on amine oxidase activity in a cell-free test system from rat liver

Code	Structure	Oxidative deamination of Spd		Oxidative deamination of Spm		Observed Category
		nkatal/mg of protein	(%)	nkatal/mg of protein	(%)	
X10		9,2	32	17,3	115	NA
X11		13,2	46	10,5	70	Inhibitor
X17		33	114	29,7	198	Activator

Spm and significantly decreased oxidation of Spd showing an ambivalent manner of action with a tendency to inhibition.

Group VI: Both benzobicyclononane derivatives X9 and X13 (Table 6) strongly increased amine oxidase activity; thereby the presence of additional phenyl fragment in X13 did not change significantly this mode of action.

Group VII: Diphenylpiperidine derivatives with two 2-hydroxyphenyl radicals (DP15 and DP18) enhanced the oxidative deamination, while those containing 4-hydroxyphenyl radicals (DP7 and DP 16) slightly inhibited PA catabolism (Table 6). This fact may reveal the significance of hydroxy-group position in the R1-phenyl ring.

Group VIII: No activators of PA oxidation were found among bacteriopurpurin derivatives (Table 7). The degree of their inhibitory effect correlates with the length of side chain radicals, where $R1 = R2$. A report of Libby et al. (1995) describes inhibitory effects of porphyrins regarding PA catabolic enzymes. Thus, the present results are consistent with these data.

Therefore, we conclude that aniline and azafluorene derivatives—groups I and III, respectively—are mainly activators, while dioxaborinopyridines and bacteriopurpurins—groups II and VIII—are very often inhibitors. The size of other groups is unfortunately rather small and further investigations are needed to conclude about a tendency. Nevertheless, here, we include all the groups for a classification model development.

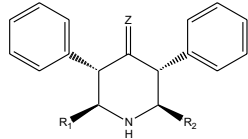
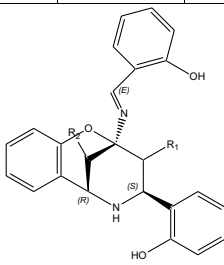
Docking

The 5LFO is a good model for exploring mammalian PA catabolic enzymes due to its structural (> 50%) and

enzymatic mode similarity to human SMO and APAO. The crystal structure of 5LFO was recently very good characterized (Sjörge et al. 2017). It is a monomer and contains an L-shaped cavity with the active site locating inside of it together with the FAD cofactor. Docking was carried out with a full conformational search for ligands (for all rotatable chemical bonds). The positions of the side chains varied for the 60 AA residues closest to the N1-acetyl-Spm molecule, i.e., their conformational adjustment for each molecule of the ligand was performed. The protein main chain and cofactor were considered rigidly fixed. In this way, several docking poses within the active site were found and stored for all 51 molecules. Further analysis was made for the lowest energy poses.

Due to some technical complications, we could not unfortunately save the figures of the best docking configurations; therefore, this part of the work provided only the calculations of interaction energies. Nevertheless, it appeared rather informative and useful. The most significant attraction between ligands and the protein was observed for 8 AAs: His64, Arg134, Glu184, Val187, Tyr204, Val206, Asp211, and Tyr430 (Supplementary Material, Table S2). Here, the most notable was His64 that interacts practically with all of the tested substances with median E_{pair} up to -18.43 kcal/mol. Other four AAs—Ser473, Cys186, Phe201, and Ser188—form less strong links with fewer ligands. Knowing that the mentioned AAs are localized in the very catalytical site of the enzyme, we can speak about the location of the ligands inside the L-shaped cavity of the murine PAO. Four of the listed AAs—His64, Tyr430, Val187, and Ser473—participate in the substrate fixation during the catalytical process. It was earlier shown that His64 is the most catalytically important as together with Tyr430 it engages in

Table 6 Structure of diphenylpiperidine (group VI) and benzobicyclononane (group VII) derivatives and their influence on amine oxidase activity in a cell-free test system from rat liver

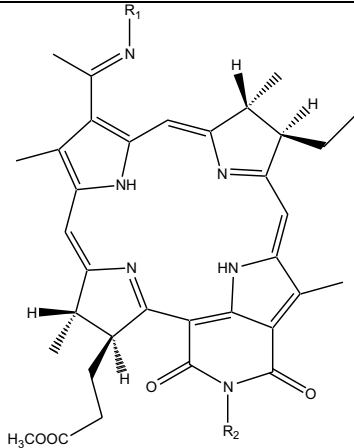
<div style="text-align: center;">  </div> <p style="text-align: center;">Group VI</p>								
Code	=Z (-Z)	R ₁	R ₂	Oxidative deamination of Spd		Oxidative deamination of Spm		Observed Category
				nkatal/mg of protein	(%)	nkatal/mg of protein	(%)	
DP7	=O	4-hydroxy-5-nitrophenyl	4-hydroxy-5-nitrophenyl	18,8	65	15,1	101	NA
DP15	-OH	2-hydroxyphenyl	2-hydroxyphenyl	43,2	149	37	247	Activator
DP16	=O	4-hydroxyphenyl	4-hydroxyphenyl	26	90	14,2	95	Inhibitor
DP18	=O	2-hydroxyphenyl	2-hydroxyphenyl	52,6	181	39	260	Activator
<div style="text-align: center;">  </div> <p style="text-align: center;">Group VII</p>								
Code	R ₁	R ₂	Oxidative deamination of Spd		Oxidative deamination of Spm		Observed Category	
			nkatal/mg of protein	(%)	nkatal/mg of protein	(%)		
X9	H	4-hydroxyphenyl	36	124	35	233	Activator	
X13	Phenyl	Phenyl	38,2	132	35	233	Activator	

lining a narrow groove in which the substrate *N*1-acetyl-Spm is placed. According to Sjögren, the secondary amine N5 of the substrate is localized between these two AAs and is likely to form hydrogen bonds with their Ne2 and OH group, respectively, which enables its positioning directly above the cofactor FAD. Val187 and Ser473 are also involved in the substrate fixation within the enzyme cavity making hydrogen bonds with its N10. The negatively charged Glu184 helps to route the positively charged substrate to the binding site inside the cavity. Tyr204 flanks the entrance of the L-shaped cavity. Asp211 is considered to be implemented in maintenance of the overall structure of the enzyme making hydrogen bonds simultaneously with His64 and Gly65 and thus participating in the hydrogen-bond network (Sjögren et al. 2017).

We applied non-parametric statistical methods for the analysis of the data to find out if there are any differences in strength of binding of activators, inhibitors, and “NA” compounds with some certain AAs in the active site (Supplementary material, Table S3). These differences were

significant for Glu184 and Asp211. The interactions of the compounds with Glu184 were not too strong, and could be useful mainly to differentiate between inhibitors and ambivalent compounds. By contrast, Asp211 was capable to form stronger bonds and was helpful to distinguish all three groups from one another (see Table 8). A significant correlation with $R = -0.35$, $P = 0.013$ revealed a pattern in a row I-NA-A. In particular, it means that while passing from inhibitor through intermediate state to activator the absolute energy value of interaction between tested compound and Asp211 increases.

The fact that inhibitors and activators bind with different energy with Asp211 seems very interesting, because this very AA as it was mentioned above is implemented in maintenance of the whole enzyme structure. Asp211 was also reported to play a role in the mechanism of enzyme inhibition by a well-known irreversible APAO inhibitor MDL72527. MDL72527 binds covalently with the cofactor leading to a flip of the His64, its moving away from Asp211 and loss of hydrogen bond between these two

Table 7 Structure of bacteriopurpurine derivatives (group VIII) and their influence on amine oxidase activity in a cell-free test system from rat liver


Group VIII

Code	R ₁ =R ₂	Oxidative deamination of Spd		Oxidative deamination of Spm		Observed Category
		nkatal/mg of protein	(%)	nkatal/mg of protein	(%)	
BP1	OH	18,7	94	9,78	94	Inhibitor
BP2	CH ₃ O	21,3	106	6,38	61	NA
BP3	C ₃ H ₇ O	11,9	60	8,50	82	Inhibitor
BP4	C ₄ H ₉ O	6,97	35	3,40	33	Inhibitor

Table 8 Comparison of the interactions with Asp211 between groups of activators, inhibitors, and NA compounds with a non-parametric method

	Inhibitor	NA	Activator	Comparison between groups <i>P</i> K–W	Correlations				
					P I-NA	P I-A	P NA-A	<i>r</i>	<i>P</i>
Gly209	0 (0...0)	0 (0...0)	0 (–0.59...0)	0.019*	0.893	0.025*	0.038*	–0.36	0.010*
Asp211	–4.59 (–5.77...–2.14)	–5.24 (–6.43...–2.02)	–7.23 (–10.52...–3.79)	0.032*	0.664	0.025*	0.028*	–0.35	0.013*

Variables were described as median and interquartile range: Me (IQR)

Comparisons between groups were made by Kruskal–Wallis rank sum test

Comparisons between groups were performed using the Mann–Whitney *U* test with correction for multiple testing according to Bonferroni method

Comments **P* < 0.05

AAs. Taken together, these facts may contribute to clarifying the role of Asp211 and His64 in catalytic process as well as help in structure-based search of active molecular agents revealing a desirable mode of their interaction with the enzyme.

It seems to be worth noticing that almost none of ligands interacted with Lys315 that is involved in the reaction of reduced FAD cofactor with oxygen. Some kind of interaction was shown only for few inhibitors.

Further analysis of partial energies (E_{Pair}) of the interaction of tested compounds with AA residues and cofactor was made. Interactions as well as hydrogen bonds with absolute values of E_{Pair} ≥ 2.5 kcal/mol were used as docking

descriptors. Statistical estimates were applied for further analysis of docking results.

Construction of a classification model on the basis of in silico and in vitro data

The preliminary statistical processing only revealed few statistically significant differences in binding of activators, inhibitors, and those compounds that were classified as NA with certain AAs in the active site (Supplementary material, Table S2). These differences were evaluated in Kruskal–Wallis test and were shown significant for Tyr127, Glu184, Phe201, Gly209, Asp211, Phe471, and Tyr472. The

further analysis was performed as classification tree building which enabled to differentiate between activators and inhibitors on the basis of their mode of binding with PA catabolic enzyme.

Descriptors of docking (AA residues with an absolute value of the attraction or repulsion energy of Epair more than 2.5 kcal/mol and hydrogen bonds with an energy of 2.5 kcal/mol, interaction with the cofactor) served to create this model according to the principle of constructing binary classification trees. According to their biological activity with respect to PA oxidation, two groups of substances—activators (19 compounds) and inhibitors (17 compounds)—were identified. The independent variables in this recognition model were descriptors of docking. A satisfactory binary classification tree enabling to distinguish between activators and inhibitors was constructed with just two descriptors, namely Asp211 and Tyr204, that were selected during the initial analysis of 54 variables (Supplementary material, Table S4). The basic classification characteristics of the tree are presented in Table 9. The first step divided the total set of the tested compounds into two mixed branches and revealed the key role of Asp211 in differentiating between inhibitors and activators (Fig. 1, Supplementary Material Fig. S3). The threshold value here was the binding energy value equal to -6.05 kcal/mol. Those compounds that gave interaction with Epair ≤ -6.05 were classified as activators and formed the node 1. This node is a mixed one and contains 16 activators (81.1%) and 3 inhibitors (18.8%). Among the correctly recognized agents there were representatives of group I—halogenated aniline derivatives B4, B6, B9, B14, two compounds from group II—CoA1 and CoA11, azafluorene derivatives of group III entirely—F1–F4, and two benzobicyclonanes from group VI. The next step

Table 9 Classification results

Actual categories	Predicted by classification and regression tree	
	Inhibitor (negative result)	Activator (positive result)
Inhibitor	14	3
Activator	3	16

Sensitivity (correct recognition of activators) 84.2%

Specificity (correct recognition of inhibitors) 82.4%

Positive predictive value 84.2%

Negative predictive value 82.4%

Accuracy 83.3%

Matthew correlation coefficient (phi-measure) 0.66

Gamma measure 0.92

Odds ratio 24.9 (95% CI 24.9–143.8)

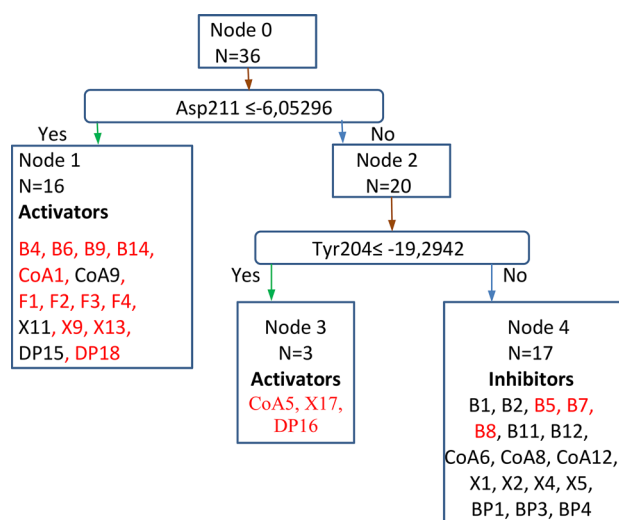


Fig. 1 Classification tree for the differentiation of activators and inhibitors of PA catabolism, built on the basis of docking results; the two amino acid residues are descriptors of docking. The classification tree was built by combining the docking and in vitro results and helps to distinguish activators from inhibitors by their mode of binding with the target enzyme. The tree includes three levels and three terminal nodes. The most populated nodes are node 1 (activators) and 4 (inhibitors). The first step divided the total set of the tested compounds into two mixed branches and revealed the key role of Asp211 in differentiating between inhibitors and activators. The next step accounting for the second descriptor Tyr204 made it possible to separate three additional substances, which, in the first step, were falsely classified as inhibitors

accounting for the second descriptor Tyr204 made it possible to separate three additional substances, which in the first step were falsely classified as inhibitors. These agents are characterized by the lowest Tyr204-binding energies—dioxaborinopyridine CoA5, azacrown ether X17, and diphenylpiperidine DP16 and form the node 3. However, node 4 also contains three falsely classified activators.

In general, the tree gave not too good but satisfactory classification of the compounds into activators and inhibitors. However, it is precious that already in the first step, the tree chose the descriptor Asp211, which was well distinguished in simple statistical comparisons, and it could be well explained biochemically. Summing up, activators can be substances with a binding energy value with Asp211 less than -6 kcal/mol or with Tyr204 less than -19.3 kcal/mol. Otherwise, the substance will be either neutral or inhibitor.

As the first node of the decision tree used Asp211, we also tested its prediction capacity with the help of ROC analysis (Fig. 2). Area under curve was 0.72 (95% CI 0.55–0.89), $P=0.025$. The highest sum of specificity and sensitivity was 1.5 at the cut-off value equal -6.05 ($Sp=0.82$, $Se=0.68$). The best cut-off value achieved by the ROC -analysis was the same as the one found out by C&RT algorithm. Thus, it can be concluded that these two different methods (C&RT

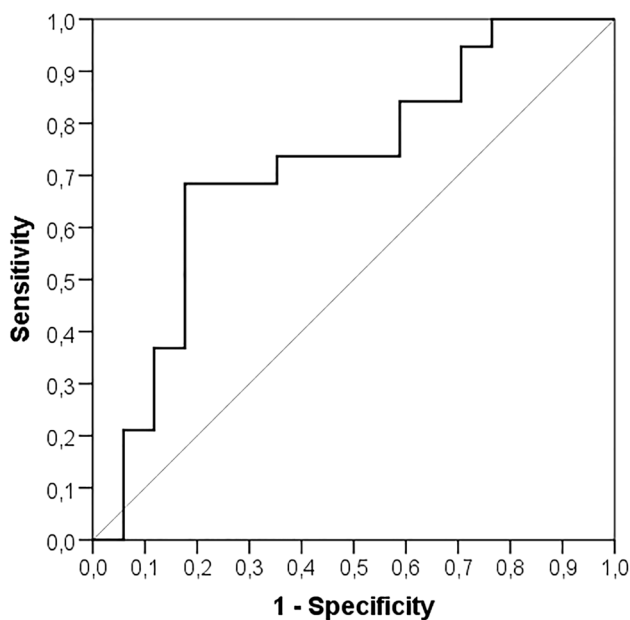


Fig. 2 ROC curve for Asp211. Area under curve was 0.72 (95% CI 0.55–0.89), $P=0.025$. The highest sum of specificity and sensitivity was 1.5 at the cut-off value equal -6.05 ($Sp=0.82$, $Se=0.68$). The best cut-off value of the binding energy with Asp211 achieved by the ROC analysis was the same as it was found out by C&RT algorithm

and ROC) support the key role of Asp211 in differentiation of the compounds.

The triad His64, Asp211 and Gly65 of murine APAO is described as corresponding to His67, Asn195, and Asp94 of yeast FMS1 (Sjögren et al. 2017). Adachi and co-authors investigated the mutated N195A and D94N forms of FMS1 and found the reduction of activity in such enzymes (Adachi et al. 2012). This effect was attributed to the role of Asn195, and Asp94 in correct positioning of the substrate for the oxidation. In this regard, making parallels with murine APAO gives an additional argument for the importance of Asp211 in catalytic process, although it is not clear yet how it is performed in the presence of the tested compounds that behave as activators.

Taken together, these results reveal the crucial AA residues binding with which determines activating effect of a ligand. On the other hand, the number of compounds in this row of structures is not enough for making the final conclusions.

The representatives of groups II, IV, and VIII are bulky; therefore, they need a larger space to fit in the available enzyme cavities. By contrast, azafluorenes have the most compact structures and can ideally fit inside the thin part of the active site of the enzyme. At the same time, they demonstrate a stable though not the strongest activating effect upon PA catabolism *in vitro*. Similar order of things is observed for aniline derivatives, most of which are also

activators. Their small size and short flexible chains allow them to locate inside the cavity.

Taken together, these results allow concluding that the location of a compound within the active site is determined by its structure and serves a background for its biological action.

Well-documented inhibitors of APAO such as guazatine and MDL 72527 and inhibitors of SMO BENSpm, CPENSpm, as well as certain pharmaceutical agents such as chlorhexidine and metocramine were docked with APAO, SMO and FMS1 (Adachi et al. 2012; Bianchi et al. 2006; Cervelli et al. 2010, 2013; Di Paolo et al. 2019). Looking at their structure, one can easily see that all these compounds are long-chained flexible aliphatic structures which follow the path of the L-shaped catalytic tunnel. Guanidino-groups are considered significant for inhibitory effect. Instead, the activators of PA oxidation explored in our work are characterized by compact condensed aromatic structures (azafluorenes) or by relatively short $-N-C-C-CO-$ fragments between two phenyl rings (anilines). Dioxaborinopyridine derivatives are mainly inhibitors being more rigid, bulky, and containing two condensed aliphatic heterocycles—one with a nitrogen atom and another one with $-O-B-O-$ fragment. Therefore, we conclude that developing a potential activator of PA catabolism should be carried out with attention to the following statements: (1) the decisive factors are size and geometric shape; (2) adding the halogens to the core structure improves or at least does not reduce the PA catabolic activating power of the substances with proper size and shape.

Conclusion

A variety of heterocyclic nitrogen-containing compounds having polyamine-like fragments were selected in search for PA metabolism modulators. Computer modeling of the ligand binding to murine PAO 5LFO made it possible to establish visually the location of molecules of a certain class within the cavity of the enzyme. The low-energy conformations for all groups of compounds are found in the same region of the active site to which the substrate binds, which confirms their potential ability to replace natural PAs in metabolic reactions. The obtained data indicate that the key residues for ligand binding in the active site of the 5LFO molecule are His64, Arg134, Glu184, Val187, Tyr204, Val206, Asp211, and Tyr430.

According to their effect on PA degradation, the compounds in this study may be classified as presumably carcinogenic and antiproliferative. Substances that inhibit oxidative deamination show probable carcinogenic properties. This category includes most of the derivatives of dioxaborinopyridine (group II) and bacteriochlorin (group VII),

as well as the molecules X1, X2, X4, X10, and X11 from the derivatives of azacrown ethers (group IV). Conversely, chemical compounds that activate di- and polyamine oxidase may become potential antitumour agents. These are aniline derivatives (group I) B4, B5, B6, B8, B9, and B14; derivatives of benzobicyclononane (group VI) X9, X13, and diphenylpiperidine (group VII) DP15, DP18.

Combining the results of in vitro screening for amine oxidase activity and docking with 5LFO, a binary classification tree was proposed that allows one to predict the character of ligand activity based on its partial binding energies with the two AA residues (Asp211 and Tyr204) of the enzyme. The determining factor of the action will be first of all the strength of interaction with Asp211. Such a model can serve as a basis for the synthesis of new modulators of PA metabolism. Thus, the docking studies help in understanding the intimate mechanism of ligand–protein interaction and structure–activity relationship.

Acknowledgements This work was financially supported by the Ministry of Education and Science of the Russian Federation (the Agreement No 02.A03.21.0008) and by the “RUDN University Program 5-100”. Docking studies were supported by Tomsk Polytechnic University Competitiveness Enhancement Program Grant No. CEP—N. Kizhner Center—213/2018. The authors thank the “International Polyamine Foundation, ONLUS” for the availability to look up in the Polyamines documentation.

Author contributions All authors listed have contributed to the conception, design, gathering, analysis, or interpretation of data, and have contributed to the writing and intellectual content of the article. All authors gave informed consent to the submission of this manuscript.

Data availability The data sets used and/or analyzed during the current study are available from the corresponding author on reasonable request.

Compliance with ethical standards

Conflict of interest All the authors confirm the permission for this publication and declare no conflict of interests.

Ethics approval and research involving human participants and/or animals All applicable international, national, and/or institutional guidelines for the care and use of animals were followed. The experiments with the animals were carried out according to the protocols approved by the Ethic Committee of PFUR (protocol no. 17/09-2015). This study does not contain any studies with human participants performed by any of the authors.

References

- Adachi MS, Juarez PR, Fitzpatrick PF (2010) Mechanistic studies of human spermine oxidase: kinetic mechanism and pH effects. *Biochemistry* 49(2):386–392. <https://doi.org/10.1021/bi9017945>
- Adachi MS, Taylor AB, Hart PJ, Fitzpatrick PF (2012) Mechanistic and structural analyses of the roles of active site residues in the yeast polyamine oxidase Fms1: characterization of the N195A and D94N Enzymes. *Biochemistry* 51(43):8690–8697. <https://doi.org/10.1021/bi3011434>
- Amendola R, Cervelli M, Fratini E, Sallustio DE, Tempera G, Ueshima T, Mariottini P, Agostinelli E (2013) Reactive oxygen species spermine metabolites generated from amine oxidases and radiation represent a therapeutic gain in cancer treatments. *Int J Oncol* 43(3):813–820. <https://doi.org/10.3892/ijo.2013.2013>
- Anderson AC (2012) Structure-based functional design of drugs: from target to lead compound. *Methods Mol Biol* 823:359–366. https://doi.org/10.1007/978-1-60327-216-2_23
- Anh LT, Polyanskii KB, Andresyuk AN, Soldatenkov AT, Mamrybekova ZhA, Kuleshova LN, Khrustalev VN (2004) Synthesis and molecular structure of 2,4,8a-triaryl-6-methylperhydro[1,3,2]dioxaborinino [5,4-c] pyridines. *Russ Chem Bull Int Ed* 53(4):842–845
- Anh LT, Hieu TH, Soldatenkov AT, Kolyadina NM, Khrustalev VN (2012a) 24-Acetyl-8,11,14-trioxa-24,27-diazapentacyclo-[19.5.1.122,26.02,7.015,20] octacos-2,4,6,15(20),16,18-hexaen-28-one. *Acta Crystallogr A* E68:o2165–o2166
- Anh LT, Hieu TH, Soldatenkov AT, Kolyadina NM, Khrustalev VN (2012b) Dimethyl 2-[22,24-dimethyl-23-oxo-8,11,14-trioxa-25-azatetracyclo [19.3.1.02,7.015,20] pentacos-2,4,6,15(20),16,18-hexaen-25-yl]but-2-enedioate. *Acta Crystallogr A* E68:o1588–o1589
- Anh LT, Hieu TH, Soldatenkov AT, Soldatova SA, Khrustalev VN (2012c) Dimethyl 2-(23-oxo-22,24-diphenyl-8,11,14-trioxa-25-azatetracyclo [19.3.1.02,7.015,20] pentacos-2,4,6,15(20),16,18-hexaen-25-yl)but-2-enedioate. *Acta Crystallogr A* E68:o1386–o1387
- Battu MB, Chandra AM, Sriram D, Yogeewari P (2014) Pharmacophore-based 3DQSAR and molecular docking studies to identify new non-peptidic inhibitors of cathepsin S. *Curr Med Chem* 21(16):1910–1921. <https://doi.org/10.2174/09298673113206660275>
- Bianchi M, Polticelli F, Ascenzi P, Botta M, Federico R, Mariottini P, Cona A (2006) Inhibition of polyamine and spermine oxidases by polyamine analogues. *FEBS J* 273(6):1115–1123. <https://doi.org/10.1111/j.1742-4658.2006.05137.x>
- Bradford MM (1976) A rapid and sensitive method for the quantitation of microgram quantities of protein utilizing the principle of protein-dye binding. *Anal Biochem* 72:248–254
- Casero RA Jr, Frydman B, Stewart TM, Woster PM (2005) Significance of targeting polyamine metabolism as an antineoplastic strategy: unique targets for polyamine analogues. *Proc West Pharmacol Soc* 48:24–30 (review)
- Cervelli M, Bellavia G, Fratini E et al (2010) Spermine oxidase (SMO) activity in breast tumor tissues and biochemical analysis of the anticancer spermine analogues BENSpm and CPENSpm. *BMC Cancer* 10:555. <https://doi.org/10.1186/1471-2407-10-555>
- Cervelli M, Polticelli F, Fiorucci L, Angelucci E, Federico R, Mariottini P (2013) Inhibition of acetyl polyamine and spermine oxidases by the polyamine analogue chlorhexidine. *J Enzym Inhib Med Chem* 28(3):463–467. <https://doi.org/10.3109/14756366.2011.650691>
- Cervelli M, Pietropaoli S, Signore F, Amendola R, Mariottini P (2014) Polyamines metabolism and breast cancer: state of the art and perspectives. *Breast Cancer Res Treat* 148(2):233–248. <https://doi.org/10.1007/s10549-014-3156-7>
- Di Paolo ML, Cervelli M, Mariottini P et al (2019) Exploring the activity of polyamine analogues on polyamine and spermine oxidase: methoctramine, a potent and selective inhibitor of polyamine oxidase. *J Enzym Inhib Med Chem* 34(1):740–752. <https://doi.org/10.1080/14756366.2019.1584620>
- Grancara S, Zonta F, Ohkubo S, Brunati AM, Agostinelli E, Toninello A (2015) Pathophysiological implications of mitochondrial oxidative

- stress mediated by mitochondriotropic agents and polyamines: the role of tyrosine phosphorylation. *Amino Acids* 47(5):869–883. <https://doi.org/10.1007/s00726-015-1964-7>
- Handa AK, Fatima T, Mattoo AK (2018) Polyamines: bio-molecules with diverse functions in plant and human health and disease. *Front Chem* 6:10. <https://doi.org/10.3389/fchem.2018.00010>
- Hieu TH, Anh LT, Soldatenkov AT, Kolyadina NM, Khrustalev VN (2012a) Dimethyl 2-[24-acetyl-28-oxo-8,11,14-trioxa-24,27-diazapentacyclo [19.5.1.1.22,26.02,7.015,20] octa-cosa-2,4,6,15(20),16,18-hexaen-27-yl] but-2-enedioate. *Acta Crystallogr A* E68:o2431–o2432
- Hieu TH, Anh LT, Soldatenkov AT, Kurilkin VV, Khrustalev VN (2012b) Meso-(1S*,21R*)-25-Methyl-8,11,14-trioxa-22,24,25-triazatetrayclo[19.3.1.02,7.015,20] penta-cosa-2,4,6,15(20),16,18-hexaene-23-thione chloroform monosolvate. *Acta Crystallogr A* E68:o2848–o2849
- Hieu TH, Anh LT, Soldatenkov AT, Vasil'ev VG, Khrustalev VN (2013) Ethyl 23-benzyl-8,11,14-trioxa-23,28,29-triazapentacyclo-[19.7.1.02,7.015,20.022,27] nonacosa-2,4,6,15(20),16,18,21,26-octaene-26-carboxylate. *Acta Crystallogr A* E69:o565–o566
- Kaur P, Chamberlin AR, Poulos TL, Sevrioukova IF (2016) Structure-based inhibitor design for evaluation of a CYP3A4 pharmacophore model. *J Med Chem* 59(9):4210–4220. <https://doi.org/10.1021/acs.jmedchem.5b01146>
- Khlebnikov AI, Schepetkin IA, Kirpotina LN, Brive L, Dahlgren C, Jutila MA, Quinn MT (2012) Molecular docking of 2-(benzimidazol-2-ylthio)-*N*-phenylacetamide-derived small-molecule agonists of human formyl peptide receptor 1. *J Mol Model* 18(6):2831–2843. <https://doi.org/10.1007/s00894-011-1307-x>
- Libby PR, Munson BR, Fiel RJ, Porter CW (1995) Cationic porphyrin derivatives as inhibitors of polyamine catabolism. *Biochem Pharmacol* 50(9):1527–1530
- Madeira F, Madhusoodanan N, Lee J, Tivey ARN, Lopez R (2019) Using EMBL-EBI services via web interface and programmatically via web services. *Curr Protoc Bioinform*. <https://doi.org/10.1002/cpbi.74>
- Meanwell NA (2018) Fluorine and fluorinated motifs in the design and application of bioisosteres for drug design. *J Med Chem*. <https://doi.org/10.1021/acs.jmedchem.7b01788>
- Miller-Fleming L, Olin-Sandoal V, Campbell K, Ralser M (2015) Remaining mysteries of molecular biology: the role of polyamine metabolites in the cell. *J Mol Biol* 427(21):3389–3406. <https://doi.org/10.1016/j.jmb.2015.06.020>
- Moschou PN, Roubelakis-Angelakis KA (2014) Polyamines and programmed cell death. *J Exp Bot* 65(5):1285–1296. <https://doi.org/10.1093/jxb/ert373>
- Murray-Stewart T, Ferrari E, Xie Y, Yu F, Marton LJ, Oupicky D, Casero RA (2017) Biochemical evaluation of the anticancer potential of the polyamine-based nanocarrier Nano11047. *PLoS One* 12(4):e0175917. <https://doi.org/10.1371/journal.pone.0175917>
- Obakan P, Arisan ED, Calcabrin A, Agostinelli E, Bolkent S, Palavan-Unsal N (2014a) Activation of polyamine catabolic enzymes involved in diverse responses against epibrassinolide-induced apoptosis in LNCaP and DU145 prostate cancer cell lines. *Amino Acids* 46(3):553–564. <https://doi.org/10.1007/s00726-013-1574-1>
- Obakan P, Arisan ED, Özfiliz P, Çoker-Gürkan A, Palavan-Ünsal N (2014b) Purvalanol A is a strong apoptotic inducer via activating polyamine catabolic pathway in MCF-7 estrogen receptor positive breast cancer cells. *Mol Biol Rep* 41(1):145–154. <https://doi.org/10.1007/s11033-013-2847-1>
- Panidthananon W, Chaowasku T, Sritularak B, Likhitwitayawuid K (2018) A new benzophenone *C*-glucoside and other constituents of pseuduvaria fragrans and their α -glucosidase inhibitory activity. *Molecules* 23(7):1600. <https://doi.org/10.3390/molecules23071600> (Published 2018 Jul 2)
- Reinus B, Kerwin SM (2019) Preparation and utility of *N*-alkynyl azoles in synthesis. *Molecules* 24(3):422. <https://doi.org/10.3390/molecules24030422>
- Samasil K, Lopes de Carvalho L, Mäenpää P, Salminen TA, Incharoen-sakdi A (2017) Biochemical characterization and homology modeling of polyamineoxidase from cyanobacterium *Synechocystis* sp. PCC 6803. *Plant Physiol Biochem* 119:159–169. <https://doi.org/10.1016/j.plaphy.2017.08.018>
- Sjögren T, Wassvik CM, Snijder A, Aagaard A, Kumanomidou T, Barlund L, Kaminski TP, Kashima A, Yokota T, Fjellström O (2017) The structure of murine *N*1-acetylspermine oxidase reveals molecular details of vertebrate polyamine catabolism. *Biochemistry* 56(3):458–467. <https://doi.org/10.1021/acs.biochem.6b01140>
- Sliwoski G, Kothiwale S, Meiler J, Lowe EW Jr (2013) Computational methods in drug discovery. *Pharmacol Rev* 66(1):334–395. <https://doi.org/10.1124/pr.112.007336>
- Storer RJ, Ferrante A (1998) Hydrogen peroxide assay for amine oxidase activity. In: Morgan DML (ed) *Methods in molecular biology: polyamine protocols*, vol 79. Humana Press, Totowa, pp 59–68
- Syatkin SP, Berezov TT (1982) Metabolism of polyamines in malignant tumors. *Bull Acad Med Sci USSR* 3:10–21 (in Russian)
- Syatkin SP, Galaev YV (1977) Oxidation of putrescine, spermidine and spermine by mouse liver diaminoxidase. *Biochemistry* 42(6):1010–1013 (in Russian)
- Syatkin SP, Kirichuk AA, Soldatenkov AT, Kutyakov SV, Neborak EV, Shevkun NA, Kuznetsova OM, Skorik AS, Terent'ev AA (2017) Screening of some dioxaborinopyridine and aniline derivatives for carcinogenic properties using a model cell-free system of regenerating rat liver. *Bull Exp Biol Med* 162:801. <https://doi.org/10.1007/s10517-017-3717-y>
- Tavloraki P, Cervelli M, Antonangeli F, Minervini G, Stano P, Federico R, Mariottini P, Polticelli F (2011) Probing mammalian spermine oxidase enzyme–substrate complex through molecular modeling, site-directed mutagenesis and biochemical characterization. *Amino Acids* 40:1115. <https://doi.org/10.1007/s00726-010-0735-8>
- Thomas TJ, Thomas T (2018) Cellular and animal model studies on the growth inhibitory effects of polyamine analogues on breast cancer. *Med Sci* 6(1):24. <https://doi.org/10.3390/medsci6010024>
- Volkov SV, Kutyakov SV, Levov AN, Polyakova EI, Le Tuan An, Soldatova SA, Terentyev PB, Soldatenkov AT (2007) Conversion of 3-benzoyl-1-methyl-4-phenyl- γ -piperidol under the action of arylamines and arylhydrazines. Synthesis of 3-arylamino-1-oxo-1-phenylpropanes and 1,3-diarylpiperidines and their fragmentation under electron impact. *Chem Heterocycl Compd* 4:544–554
- Vucicevic J, Nikolic K, Mitchell JBO (2017) Rational drug design of antineoplastic agents using 3D-QSAR, cheminformatic, and virtual screening approaches. *Curr Med Chem*. <https://doi.org/10.2174/0929867324666170712115411>
- Wallace HM, Duthie J, Evans DM, Lamond S, Nicoll KM, Heys SD (2000) Alterations in polyamine catabolic enzymes in human breast cancer tissue. *Clin Cancer Res* 6(9):3657–3661
- Wang Q, Wang Y, Wang K, Yang J, Cao C (2015) Polyamine analog TBP inhibits proliferation of human K562 chronic myelogenous leukemia cells by induced apoptosis. *Oncol Lett* 9:278–282. <https://doi.org/10.3892/ol.2014.2615>
- Wang J, Li T, Zang L, Pan X, Wang S, Wu Y, Wang G (2017) Apigenin inhibits human SW620 cell growth by targeting polyamine catabolism. *Evid Based Complement Altern Med* 2017:3684581. <https://doi.org/10.1155/2017/3684581>

Publisher's Note Springer Nature remains neutral with regard to jurisdictional claims in published maps and institutional affiliations.